PERFORMANCE POTENTIAL OF ORC ARCHITECTURES FOR WASTE HEAT RECOVERY TAKING INTO ACCOUNT DESIGN AND ENVIRONMENTAL CONSTRAINTS

S. Lecompte*, M. van den Broek, M. De Paepe

Department of Flow, Heat and Combustion Mechanics,
Ghent University, Sint-Pietersnieuwstraat 41, 9000 Gent, Belgium
Steven.lecompte@UGent.Be, Martijn.vandenBroek@UGent.Be, Michel.DePaepe@UGent.Be

* Corresponding Author

ABSTRACT

The subcritical ORC (SCORC), sometimes with addition of a recuperator, is the de facto state of the art technology in the current market. However architectural changes and operational modifications have the potential to improve the base system. The ORC architectures investigated in this work are: the transcritical ORC (TCORC), the triangular cycle (TLC) and the partial evaporation ORC (PEORC). Assessing the potential of these cycles is a challenging topic and is brought down to two steps. First, the expected thermodynamic improvement is quantified by optimizing the second law efficiency. Secondly, the influences of technical constraints concerning volumetric expanders are investigated. In the first step, simple regression models are formulated based on an extensive set of boundary conditions. In addition a subset of environmentally friendly working fluids is separately analysed. In the second step, two cases are investigated with the help of a multi-objective optimization technique. The results of this optimization are compared with the first step. As such the effect of each design decision is quantified and analysed, making the results of this work especially interesting for manufacturers of ORC systems.

1. INTRODUCTION

In view of increasing energy demand and environmental concerns it becomes essential to use our natural resources more efficiently. Between 1990 and 2008 the world energy use has already risen more than 40% [1]. Recovery of unused heat from industrial process is evidently an effective measure to make better use of our resources. Statistical studies show that low grade waste heat accounts for more than 50% of the total heat generated in the industry [2]. As such, many companies are interested to exploit new technologies to make valuable use of low grade waste heat.

Organic Rankine cycles (ORC) offer the possibility to generate electricity from the leftover waste heat, even with temperatures below 100°C [3]. Typical benefits associated with ORC are: autonomous operation, favorable operating pressures and low maintenance costs [4]. Waste heat applications roughly consist of up to 20% [5] of the ORC market, preceded by geothermal and biomass installations. Increasing the ORC performance would facilitate further market penetration.

At the moment, most commercially available ORCs have comparable design characteristics, i.e. they operate in the subcritical regime and with well accepted working fluids (WF). However, alternative cycle designs (with matching working fluids) have the potential for increased performance. Performance gains over the subcritical ORC (SCORC) are reported for, amongst others, multi-pressure cycles (MP) [6-9], triangular cycles (TLC) [10-12], cycles with zeotropic working fluids (ZM) [13-15] and transcritical cycles (TCORC) [10, 16-19]. Three cycle configurations, the SCORC, the partial evaporation cycle (PEORC) and the TCORC, are systematically analysed in this work. The

PEORC is a hybrid between the TLC and the SCORC. The working fluid in the PEORC enters the turbine in a state between saturated liquid and saturated vapour.

Assessing the potential of these cycles is a challenging topic and is brought down to two steps. This work provides the integration of these steps and extends two previous conference papers [20, 21] by investigating the effect of limiting the working fluids to an environmentally friendly set. In anticipation of new European F-gas regulations [22] the incentive is launched to restrict the use of fluids with a Global Warming Potential (GWP) value of > 150. By 2015 this rule would apply to domestic freezers and refrigerators and by 2022 in extension to certain commercial installations. While the current rules apply for refrigerators and freezers an analogous restriction can be expected for power producing cycles.

In step one the second law efficiency is maximized. A large set of boundary conditions is considered to formulate simple regression models. These are used to compare alternative cycles in a first design iteration. To use the regression models the computational effort is low and no expert knowledge is required. In the second step, the effect of integrating volumetric expander design criteria is investigated. A multi-objective optimization is employed on two objectives: net power output and expander volume coefficient. A large computational cost is associated to this type of optimization but the cycle designer can now make the trade-off between expander sizing and cycle efficiency. In the current work, a specific case is analysed using this methodology and compared with the simple regression models from step one.

2. ALTERNATIVE ORC CYCLES

Three cycles architectures are investigated: the subcritical ORC (SCORC), the partial evaporation ORC (PEORC) and the transcritical ORC (TCORC). The cycle layout is identical for the three architectures and shown in Figure 1. The T-s diagram which introduces the nomenclature used is given in Figure 2.

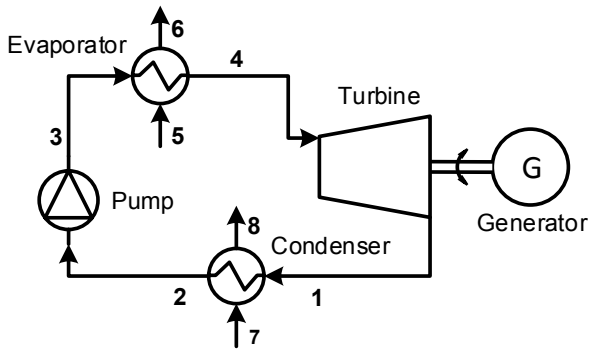

Figure 1: Basic ORC layout.

In a TCORC the evaporator is typically called a vapour generator because the two-phase state is omitted. In a TLC, only the pre-heating section remains and for the PEORC the working fluid evaporates to a state between saturated liquid and saturated vapour.

3. CASE DEFINITION

Two waste heat recovery cases are detailed in the second optimization step, see Table 1. Maximization of the ORC net power output (or second law efficiency) is key for these systems. Sometimes an artificial cooling limit is imposed to avoid condensation of flue gasses [23]. The condensed acids potentially give rise to corrosion and damage of the heat exchangers. In the investigated cases no upper cooling limit is imposed. The proposed cases and classification are based on data gathered in the ORCNext project [24].

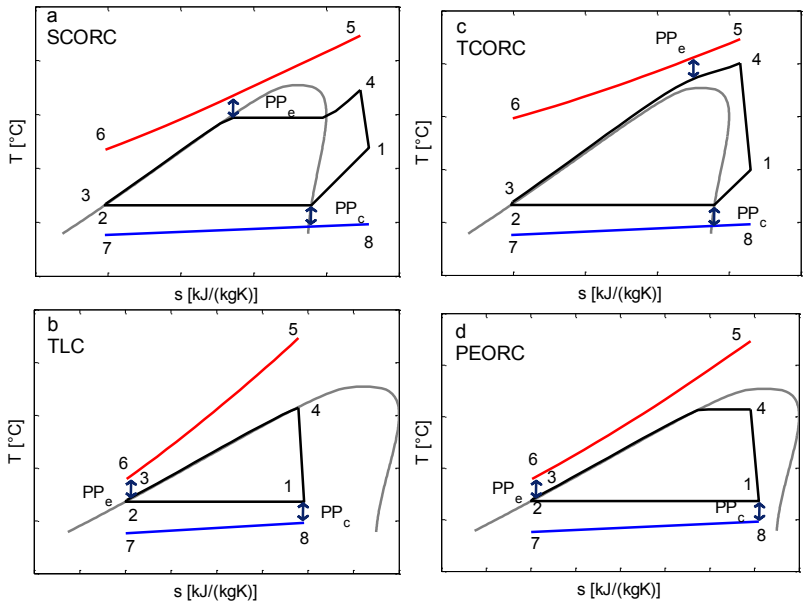

Figure 2: T-s diagrams for the SCORC, TCORC, TLC and PEORC.

Table 1: Definition of waste heat recovery cases.

Case	Case description	$T_{average}$ [°C]	Other applications
1	Flue gas from drying process	240	Exhaust gas internal combustion engines [4]
2	Flue gas from electric arc furnace	305	Cement industry [25] Exhaust gas turbine [4]

4. MODEL AND CYCLE ASSUMPTIONS

4.1 Cycle assumptions

The parameters characterizing the thermodynamic states of the ORC are shown in Table 2. The model assumes steady state operation of the system. Heat losses to the environment and pressure drops in the heat exchangers are considered negligible. No subcooling is considered. A discretization approach is implemented for modelling the heat exchangers. The evaporators are segmented into N parts to take into account changing fluid properties. Especially for the TCORC vapour generator this is essential. Details about the modelling approach are found in previous work by the authors [15, 32].

Table 2: Cycle assumptions.

Parameter	Description	Value
η_{pump}	Isentropic efficiency pump [%]	70
$\eta_{turbine}$	Isentropic efficiency turbine [%]	80
PP_e	Pinch point temperature difference in evaporator [°C]	5
PP_c	Pinch point temperature difference in condenser [°C]	5
T_5	Heat carrier inlet temperature [°C]	100-350
T_2	Cooling loop inlet temperature [°C]	15-30
ΔT_{cf}	Cooling loop temperature rise [°C]	10
$\dot{m}$	Mass flow rate heat carrier [kg/s]	1

When changing N=20 to N=100 the calculated net power output of the TCORC changes less than

0.1%. To keep the calculation time acceptable N=20 segments is chosen. The condenser is divided into three zones: superheated, condensing and subcooling zone.

Thermophysical data are obtained from CoolProp 4.2.3 [26]. Only pure working fluids are considered, working fluid mixtures are out of scope. The working fluids under consideration all have a critical temperature above 60 °C to make sure two-phase condensation occurs. As such 67 working fluids remain. For the environmentally friendly set of working fluids the ozon depletion potential should be zero and the global warming potential must be lower than 150. This results in 48 remaining working fluids.

Furthermore, for the SCORC the maximum pressure is 0.9 times the critical pressure [15,17]. This is to avoid unstable operation in near-critical conditions. For the SCORC and TCORC the expansion process should end at a superheated state. For the multi-objective optimization (STEP 2) the cooling loop inlet temperature is fixed at 20 °C.

4.2 Performance evaluation criteria

The performance evaluation criteria will only be briefly explained here as these can be found in other works of the author [14, 20, 21]. The second law efficiency is defined as:

$$\eta_{II} = \frac{\dot{W}}{\dot{I}} \tag{1}$$

With $\dot{I}$ the exergy flow:

$$\dot{I} \quad \cdot \tag{2}$$

The specific exergy e for a steady state stream, assuming potential and kinetic contributions are negligible, is given as:

$$e = h - h_o - T_0(s - s_0) \tag{3}$$

For the dead state (T_0, p_0) the condenser cooling loop inlet temperature and pressure are chosen. Performance criteria for the expanders are formulated next. In this work volumetric machines are investigated and the volumetric coefficient is used as evaluation criteria:

$$VC = \frac{v_{\exp,out}}{h_{in,\exp} - h_{out,\exp}} \tag{4}$$

The VC value is directly related to the size of the expander and permits to include general design ranges in the analysis. Realistic values of the VC in refrigeration and heat pump applications range between 0.25 and 0.6 m³/MJ [23]. In a theoretical study, Maraver et al. [23] report VC values between 0.26 and 936.50 m³/MJ for different waste heat carriers and working fluids.

5. OPTIMIZATION

When optimizing the ORC with the parameters given in Table 2 two degrees of freedom are left. Depending on the cycle types these are typically defined as:

- The superheating and evaporation pressure, for the SCORC.
- The vapour quality and evaporation pressure, for the PEORC.
- The turbine inlet temperature and supercritical pressure, for the TCORC.

In a previous paper [20] two dimensionless parameters, F_s and $F_{p,}$ were introduced. Both have a range between 0 and 1. These parameters uniquely specify the operating state of the ORC. The benefit is that these two parameters fully cover the search space considering the three cycle architectures under investigation. Their definition is given below:

$$F_p = \frac{p_{wf,e} - p_{\min}}{p_{\max} - p_{\min}} \tag{5}$$

$$p_{\max} = 1.3 p_{wf,crit} \text{ if } T_5 - PP_e > T_{wf,crit} \tag{6}$$

$$p_{\max} = p_{wf,sat}(T = T_5 - PP_e) \text{ if } T_5 - PP_e < T_{wf,crit} \tag{7}$$

$$p_{\min} = p_{wf,sat}(T = T_8 + PP_c) \tag{8}$$

$$F_s = \frac{s_4 - s_{\min}}{s_{\max} - s_{\min}} \tag{9}$$

$$s_{\min} = s_{wf,sat,liq}(p = p_{wf,e}) \text{ if } p_{wf,e} < p_{wf,crit} \tag{10}$$

$$s_{\min} = s_{wf,crit} \text{ if } p_{wf,e} > p_{wf,crit} \tag{11}$$

$$s_{\max} = s_{wf}(p = p_{wf,e}, T = T_5 - PP_e) \tag{12}$$

5.1 Maximization of η_{II} (STEP 1)

The boundary conditions for the optimization are a set T_5 = [100, 120, 140, 160, 180, 200, 225, 250, 275, 300, 325, 350] °C, T_7 = [15, 20, 25, 30] °C resulting in a total of 48 points. In each of these points a multistart algorithm [27] searches the global maximum of the second law efficiency ($\eta_{II,\max}$). First, the multistart algorithm uniformly distributes 20 initial points in the search space (F_s,F_p) for the local solver to start. Next, a local solver based on a trust-region algorithm [20] starts at these trail points and the best solution is retained. Increasing the start points to 40 gave identical results.

5.2 Multi-objective optimization of VC and η_{II} (STEP 2)

Table 3: Settings of the genetic algorithm.

Parameter	Value
Generations	100
Population size	10000
Crossover rate	0.8
Migration rate	0.2
Mutation type	Gaussian (shrink = 1, scale = 1)
Pareto fraction	0.35

The multi-objective algorithm simultaneously maximizes η_{II} and minimizes VC. The VC is constrained to a range [0.1, 6.5]. The genetic algorithm implemented is based on the NSGA-II algorithm [28]. The settings of the genetic algorithm are provided in Table 3.

6. RESULTS AND TRENDS

6.1 Regression models (STEP 1)

The environmentally friendly working fluids resulting from the optimization are given in Table 6, Table 7 and Table 8 for respectively the SCORC, TCORC and PEORC. For the initial full set of working fluids we refer to a previous paper [20] by the authors. A simple regression model of the second law efficiency can be formulated in function of the T_5 and T_7. The regression model takes the form:

$$\eta_{II,\max} = a + \frac{b(cT_7 + 1)}{(dT_5 + 1)} \tag{13}$$

Goodness of fit statistics [29], the adjusted R^2 and sum square of errors (SSE) are provided in Table 4 and can be considered highly satisfactory. The regression coefficients are given in Table 5.

Table 4: Goodness of fit statistics.

Case	Adjusted R^2	SSE
All working fluids (all WF):		
SCORC	0.9917	0.0039
TCORC	0.9873	0.0055
PEORC	0.9976	0.00056
Environmentally friendly working fluids (env. WF):		
SCORC	0.9924	0.0041
TCORC	0.9944	0.0018
PEORC	0.9976	0.00056

Table 5: Regression coefficients.

	a		b		c		d	
Case	all WF	env. WF	all WF	env. WF	all WF	env. WF	all WF	env. WF
SCORC	0.7466	0.7548	1.357	1.735	3.043	2.488	-13.07	-14.6
PEORC	0.7408	0.7408	0.4796	0.4796	3.514	3.514	-8.184	-8.184
TCORC	0.7484	0.7228	0.9866	0.3061	3.083	2.846	-10.7	-4.624

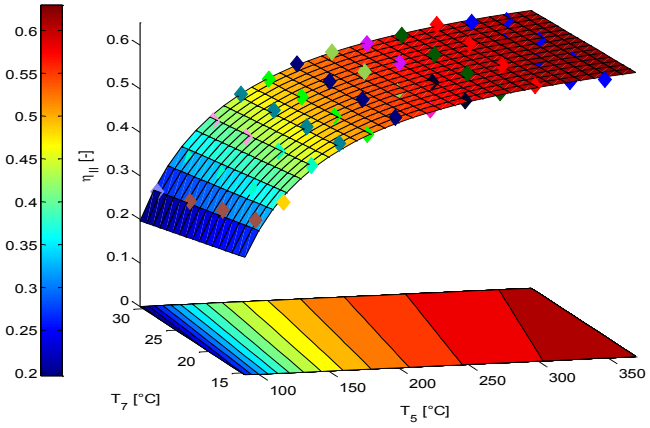

Figure 3: η_{II} optimization, full set of working fluids, surface fit for the SCORC.

For the full set of working fluids, the surface fit for the SCORC is given in Figure 3. The indicated points represent the results of the second law optimization, the colours correspond with the different working fluids. The performance benefit of the TCORC and PEORC over the SCORC are visualized in respectively Figure 4a and Figure 4b. It is clear that both the TCORC and PEORC result in increased second law efficiencies over the SCORC. An increase up to 13 % for the TCORC and 73% for the PEORC is observed at low temperatures (100 °C). However a strong dependency on the heat carrier temperatures should be noted. At high temperatures (350 °C) the relative increase in second law efficiency is reduced to around 2% and 5% for respectively the TCORC and PEORC.

When environmentally friendly working fluids are imposed, the PEORC working fluids do not change. However, as can be seen from Figure 5a (SCORC) and Figure 5b (TCORC), going to environmentally friendly working fluids results in an apparent performance decrease. Again, at low temperatures the performance decrease is the most noticeable (up to 12% for the SCORC and 6% for the TCORC). Furthermore no environmentally friendly working fluids are found for the TCORC under heat carrier inlet temperatures 100 °C and 120 °C. This indicates that there is still a gap for high performing environmentally friendly working fluids for transcritical operation.

6.2 Considering expander evaluation criteria (STEP 2)

Next we consider the effect of the expander performance criteria. As discussed in section 4.2 the VC ratio is directly related to the size of the equipment. Therefore, a multi-objective optimization is employed to simultaneously maximize η_{II} and minimize VC. Again, only the environmentally friendly set of working fluids is considered. The Pareto front for Case 1 and Case 2 are shown in Figure 6a and Figure 6b. Cyclopentane is already used in commercial ORC installations [30]. R1233ZDE is considered a low GWP alternative [31] for the well-known R245fa. Acetone is also considered a potential [32, 33] ORC working fluid.

It is clear that mainly the choice of the working fluid determines the VC. Only in second instance the operating conditions affect the relation η_{II} and VC. As expected, the optimal cycle type is always the PEORC. For Case 1 the VC varies between 0.342 (η_{II} = 0.536) and 5.957 (η_{II} = 0.635). For Case 2 the VC varies between 0.344 (η_{II} = 0.536) and 6.121 (η_{II} = 0.611).

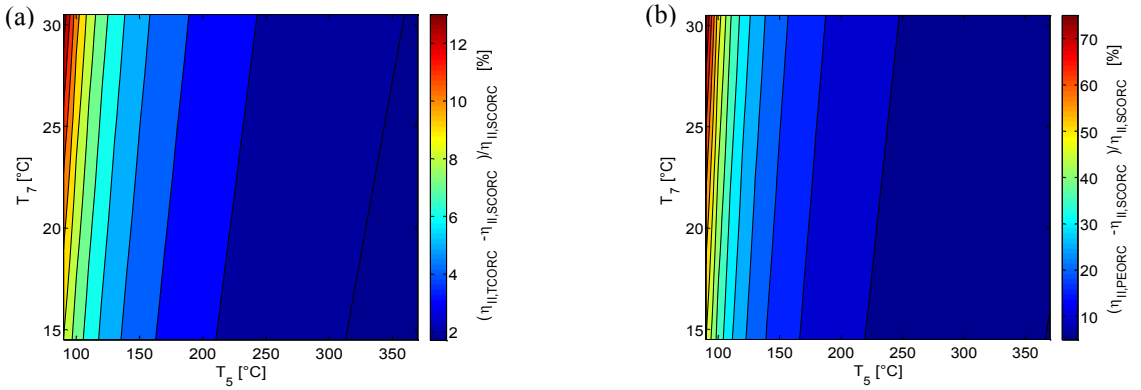

Figure 4: Relative difference η_{II} of (a) TCORC and (b) PEORC versus SCORC.

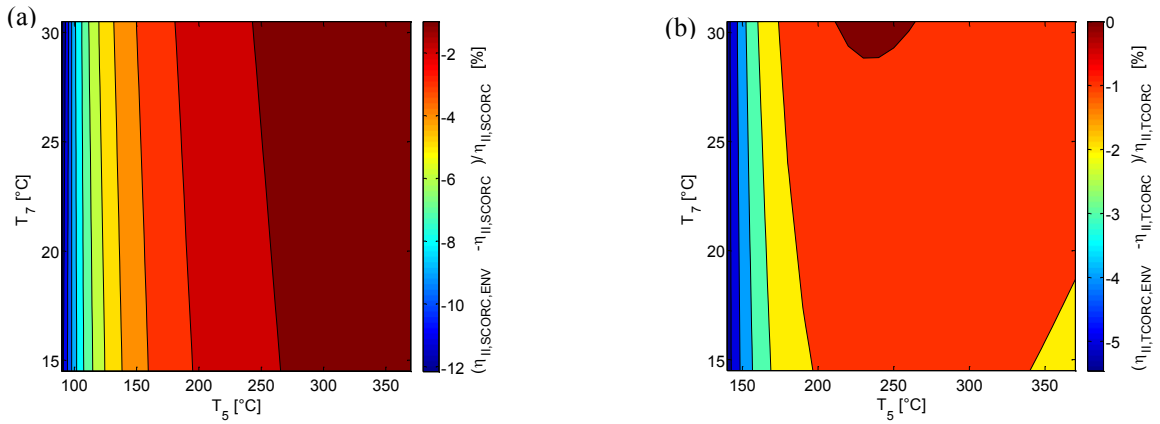

Figure 5: Relative difference η_{II} for full set versus environmentally friendly set of working fluids (a) SCORC (b) TCORC.

Table 6: SCORC environmentally friendly working fluids resulting from η_{II} maximization.

T_5|T_7 °C	15	20	25	30
100	R1234yf	R1234yf	R1234yf	R1234yf
120	R1234yf	R1234yf	R1234yf	R1234yf
140	R1234ZEE	R1234ZEE	R1234ZEE	R1234ZEE
160	R1234ZEE	R1234ZEE	R1234ZEE	Isobutane
180	Isobutane	Isobutane	Isobutane	Isobutane
200	Neopentane	Neopentane	Neopentane	Neopentane
225	R1233ZDE	R1233ZDE	R1233ZDE	R1233ZDE
250	n-pentane	n-pentane	n-pentane	n-pentane
275	Isohexane	n-Hexane	Isohexane	Cyclopentane
300	Cyclopentane	Cyclopentane	Cyclopentane	Cyclopentane
325	Acetone	Acetone	Acetone	Acetone
350	Acetone	Acetone	Acetone	Acetone

Table 7: TCORC environmentally friendly working fluids resulting from η_{II} maximization.

T_5|T_7 °C	15	20	25	30
120	R1234yf	R1234yf	R1234yf	R1234yf
140	R1234yf	R1234yf	R1234yf	R1234yf
160	R1234ZEE	R1234ZEE	R1234ZEE	R1234ZEE
180	Neopentane	Neopentane	Neopentane	Neopentane
200	Neopentane	Neopentane	Neopentane	Neopentane
225	n-pentane	n-pentane	n-pentane	n-pentane
250	n-pentane	n-pentane	n-pentane	n-pentane
275	Cyclopentane	Cyclopentane	Cyclopentane	Cyclopentane
300	Cyclopentane	Cyclopentane	Cyclopentane	Cyclopentane
325	Acetone	Acetone	Acetone	Acetone
350	Acetone	Acetone	Acetone	Acetone

Table 8: PEORC environmentally friendly working fluids resulting from η_{II} maximization.

T_5|T_7 °C	15	20	25	30
100	MD3M	MD3M	MD3M	MD3M
120	Water	MD3M	MD3M	MD3M
140	Water	Water	Water	D6
160	MD3M	D6	D6	D6
180	D4	MD2M	MD2M	MD2M
200	Water	Water	Water	D4
225	n-Dodecane	n-Dodecane	n-Dodecane	n-Dodecane
250	Water	Water	n-Dodecane	n-Dodecane
275	Water	Water	Water	Water
300	Water	Water	Water	Water
325	Water	o-xylene	o-xylene	o-xylene
350	Water	Water	Water	Water

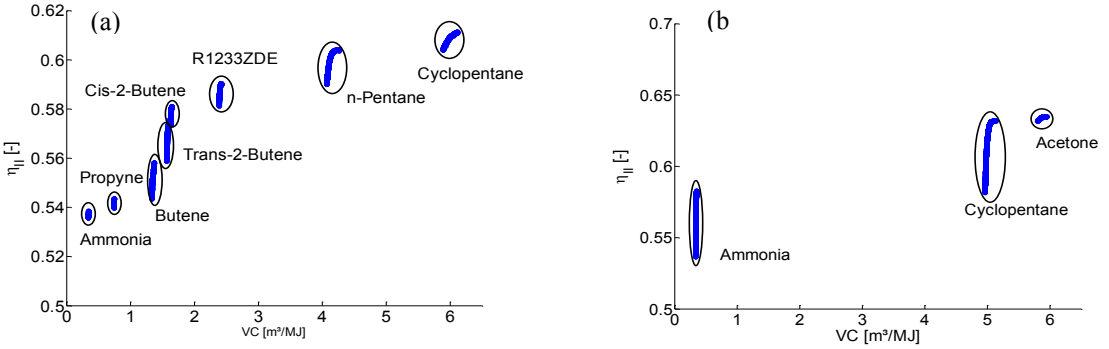

Figure 6: Pareto fronts of VC versus η_{II} for (a) Case 1 and (b) Case 2.

The results of applying the regression models from section 6.1 are given in Table 9. Considering the highest VC values, the reduction in second law efficiency is 5% for Case 1 and 4.9% for Case 2. As such, this optimization step is crucial for the ORC designer to make the final trade-off between cycle performance and expander size and complexity.

Table 9: Results of applying the regression models on the two cases (T_7 = 20°C).

η_{II}	Regression model all WF			Regression model environmentally friendly WF		
	SCORC	TCORC	PEORC	SCORC	TCORC	PEORC
Case 1	0.588	0.605	0.643	0.581	0.602	0.643
Case 2	0.625	0.638	0.667	0.621	0.634	0.667

CONCLUSIONS

- Simple regression models are formulated. These have a low computational cost and are employed to make a first assessment between the SCORC, TCORC and PEORC:
  - Compared to the SCORC, the TCORC and PEORC have a relative increase in second law efficiency of 13% and 73% for a heat carrier temperature of 100 °C

- For increasing heat carrier temperatures the performance benefit becomes lower: respectively 2% and 5% for the TCORC and PEORC with a heat carrier temperature of 350 °C.
- Considering environmentally friendly working fluids the second law efficiency is reduced with up to 12% for the SCORC and up to 6% for the TCORC. Again, for increasing heat carrier temperatures, the difference is lower.
- There is still a gap for high performing environmentally friendly working fluids for transcritical operation under low heat carrier temperatures.

- Pareto fronts of second law efficiency and volume coefficient are derived for two cases.
  - The choice of working fluid essentially determines the volume coefficient. The operating parameters have a secondary influence.
  - The second law efficiency is reduced in favour of a lower VC. For example, compared to the regression models, the second law efficiency reduces with 5% for Case 1 and 4.9% for Case 2 with the VC respectively 5.95 and 6.12.

NOMENCLATURE

η	efficiency	(–)
ν	specific volume	(–)
e	specific exergy	(kJ/kg)
F	dimensionless ORC state parameter	(–)
$\dot{m}$	mass flow rate	(kg/s)
PP	pinch point temperature difference	(°C)
TCORC	transcritical ORC	(–)
TLC	triangular cycle	(–)
SCORC	subcritical ORC	(–)
PEORC	partial evaporation ORC	(–)
V	specific volume	(m^3/kg)
VC	volume coefficient	(m^3/MJ)
$\dot{W}$	power	(kW)
Subscript		
e	evaporator	
c	condenser	
crit	critical	
hf	heat carrier	
sat	saturated	
wf	working fluid	
0	dead state	

REFERENCES

[1] International Energy Outlook 2011. U.S. Energy Information Administration2011.
[2] S. Quoilin, S. Declaye, B.F. Tchanche, V. Lemort. Thermo-economic optimization of waste heat recovery Organic Rankine Cycles. Applied Thermal Engineering. 31 (2011) 2885-93.
[3] A. Schuster, S. Karellas, E. Kakaras, H. Spliethoff. Energetic and economic investigation of Organic Rankine Cycle applications. Applied Thermal Engineering. 29 (2009) 1809-17.
[4] B.F. Tchanche, G. Lambrinos, A. Frangoudakis, G. Papadakis. Low-grade heat conversion into power using organic Rankine cycles – A review of various applications Renewable and Sustainable Energy Reviews 15 (2011) 3963 - 79.
[5] S. Quoilin, M.V.D. Broek, S. Declaye, P. Dewallef, V. Lemort. Techno-economic survey of Organic Rankine Cycle (ORC) systems. Renewable and Sustainable Energy Reviews. 22 (2013) 168-86.
[6] M. Kanoglu. Exergy analysis of a dual-level binary geothermal power plant Geothermics 31 (2002) 709 - 24.
[7] M.Z. Stijepovic, A.I. Papadopoulos, P. Linke, A.S. Grujic, P. Seferlis. An exergy composite curves approach for the design of optimum multi-pressure organic Rankine cycle processes. Energy. 69 (2014) 285-98.
[8] Z. Gnutek, A. Bryszewska-Mazurek. The thermodynamic analysis of multicycle ORC engine Energy 26 (2001) 1075 - 82.
[9] A. Franco, M. Villani. Optimal design of binary cycle power plants for water-dominated, medium-temperature geothermal fields Geothermics 38 (2009) 379 - 91.

[10] A. Schuster, S. Karellas, R. Aumann. Efficiency optimization potential in supercritical Organic Rankine Cycles Energy 35 (2010) 1033 - 9.
[11] I.K. Smith. Development of the trilateral flash cycle system Part1: fundamental considerations. Proceedings of the Institution of Mechanical Engineers, Part A: Journal of Power and Energy. (1993).
[12] J. Fischer. Comparison of trilateral cycles and organic Rankine cycles Energy 36 (2011) 6208 - 19.
[13] F. Heberle, M. Preißinger, D. Brüggemann. Zeotropic mixtures as working fluids in Organic Rankine Cycles for low-enthalpy geothermal resources. Renewable Energy. 37 (2012) 364-70.
[14] S. Lecompte, B. Ameel, D. Ziviani, M. van den Broek, M. De Paepe. Exergy analysis of zeotropic mixtures as working fluids in Organic Rankine Cycles. Energy Conversion and Management. 85 (2014) 727-39.
[15] M. Chys, M. van den Broek, B. Vanslambrouck, M.D. Paepe. Potential of zeotropic mixtures as working fluids in organic Rankine cycles Energy 44 (2012) 623 - 32.
[16] B. Saleh, G. Koglbauer, M. Wendland, J. Fischer. Working fluids for low-temperature organic Rankine cycles Energy 32 (2007) 1210 - 21.
[17] Z. Shengjun, W. Huaixin, G. Tao. Performance comparison and parametric optimization of subcritical Organic Rankine Cycle (ORC) and transcritical power cycle system for low-temperature geothermal power generation Applied Energy 88 (2011) 2740 - 54.
[18] Y.-J. Baik, M. Kim, K.C. Chang, S.J. Kim. Power-based performance comparison between carbon dioxide and R125 transcritical cycles for a low-grade heat source Applied Energy 88 (2011) 892 - 8.
[19] S. Karellas, A. Schuster, A.-D. Leontaritis. Influence of supercritical ORC parameters on plate heat exchanger design. Applied Thermal Engineering. 33–34 (2012) 70-6.
[20] S. Lecompte, H. Huisseune, M. van den Broek, M. De Paepe. Thermodynamic optimization of Organic Rankine Cycle architectures for waste heat recovery (under review). The 28th international conference on efficiency, cost, optimization, simulation and environmental impact on energy systems, Pau, France, 2015.
[21] S. Lecompte, M. van den Broek, M. De Paepe. Techno-thermodynamic optimization of organic Rankine cycle architectures for waste heat recovery. 11th International Conference on Heat Transfer, Fluid Mechanics and Thermodynamics, Kruger National Park, South Africa, 2015.
[22] The European Parliament. European Parliament legislative resolution of 12 March 2014 on the proposal for a regulation of the European Parliament and of the Council on fluorinated greenhouse gases. COM(2012)0643 – C7-0370/2012 – 2012/0305(COD)2014.
[23] D. Maraver, J. Royo, V. Lemort, S. Quoilin. Systematic optimization of subcritical and transcritical organic Rankine cycles (ORCs) constrained by technical parameters in multiple applications. Applied Energy. 117 (2014) 11-29.
[24] S. Lemmens, S. Lecompte, M. De Paepe. Workshop financial appraisal of ORC systems (ORCNext project: www.orcnext.be). 2014.
[25] J. Wang, Y. Dai, L. Gao. Exergy analyses and parametric optimizations for different cogeneration power plants in cement industry. Applied Energy. 86 (2009) 941-8.
[26] I.H. Bell, J. Wronski, S. Quoilin, V. Lemort. Pure and Pseudo-pure Fluid Thermophysical Property Evaluation and The Open-Source Thermophysical Property Library Coolprop. Industrial & Engineering Chemistry Research. 53 (2014) 2498-508.
[27] Z. Ugray, L. Lasdon, J. Plummer, F. Glover, J. Kelly, M. Rafael. Scatter Search and Local NLP Solvers, A multistart Framework for Global Optimization. INFORMS Journal on Computing. 19 (2007) 238-340.
[28] K. Deb. Multi-Objective Optimization Using Evolutionary Algorithms. Wiley2001.
[29] R.L. Mason, R.F. Gunst, J.L. Hess. Statistical Design and Analysis of Experiments. John Wiley & Sons, Inc.2003.
[30] P. Del Turco, A. Antinio, A.S. Del Greco, A. Bacci, G. Landi, G. Seghi. The ORegen™ Waste Heat Recovery Cycle: Reducing the CO2 Footprint by Means of Overall Cycle Efficiency Improvement. ASME 2011 Turbo Expo: Turbine Technical Conference and Exposition, Vancouver, British Columbia, Canada, 2011.
[31] F. Molés, J. Navarro-Esbrí, B. Peris, A. Mota-Babiloni, Á. Barragán-Cervera, K. Kontomaris. Low GWP alternatives to HFC-245fa in Organic Rankine Cycles for low temperature heat recovery: HCFO-1233zd-E and HFO-1336mzz-Z. Applied Thermal Engineering. 71 (2014) 204-12.
[32] R. Rayegan, Y.X. Tao. A procedure to select working fluids for Solar Organic Rankine Cycles (ORCs). Renewable Energy. 36 (2011) 659-70.
[33] L. Pierobon, T.-V. Nguyen, U. Larsen, F. Haglind, B. Elmegaard. Multi-objective optimization of organic Rankine cycles for waste heat recovery: Application in an offshore platform. Energy. 58 (2013) 538-49.

ACKNOWLEDGEMENT

The results presented in this paper have been obtained within the frame of the IWT SBO-110006 project The Next Generation Organic Rankine Cycles (www.orcnext.be), funded by the Institute for the Promotion and Innovation by Science and Technology in Flanders. This financial support is gratefully acknowledged.